Dielectric relaxation of calcite-type carbonate salts: Defect structure and defect dipole dynamics in polycrystalline magnesite

A. N. Papathanassiou and J. Grammatikakis
Department of Physics, Section of Solid State Physics, Panepistimiopolis, University of Athens, GR 157 84 Zografos, Athens, Greece
(Received 2 December 1996; revised manuscript received 28 March 1997)

The low-temperature thermal depolarization spectrum of polycrystalline magnesite $MgCO_3$ reveals a unique broad dipolar relaxation peak, which reaches a maximum around 140 K. The relaxation mechanism is probably related to a defect dipole population, with distribution in the relaxation time. By employing the partial heating scheme, we found the activation energy values distributing from 0.19 to 0.30 eV. Assuming a Gaussian distribution in the activation energy values, the full curve fitting led to the evaluation of the relaxation parameters $E_0=0.220$ eV, $\sigma=0.023$ eV, and $\tau_0=4.787\times10^{-6}$ s. Our results are extensively discussed in relation to those reported for the other calcite-type carbonate members; i.e., calcite ($CaCO_3$) and dolomite [$CaMg(CO_3)_2$]. The overall view of the dielectric relaxation in the calcite family materials show that each sublattice type (the calcium and the magnesium ones) favors a certain defect structure. There is strong evidence that Mn^{2+} and Sr^{2+} impurities as well as the water molecules or the hydroxyl ions are the most probable participants to the defect dipole configurations. [S0163-1829(97)06638-1]

I. INTRODUCTION

The study of the defect dipole relaxation in mixed ionic crystals, in relation to the dielectric relaxation of the end components, can provide valuable information about:

(i) The defect structure establishment (i.e., the kind of the impurities which are favored to enter into the matrix and the type of defect dipoles, which are formed, in the mixed system) in relation to the specific sublattice properties; the condition for the establishment of a certain defect structure is the minimization of the Gibbs free energy of the crystal.

(ii) The effect of the variation of the matrix to the relaxation of a certain type of defect dipoles (equivalently, to the migration process of the defects forming the dipole).[1] In the latter case, the substitution of the ions of a pure ionic crystal, which gradually leads to the creation of the mixed crystal, results in the change of the lattice constant. The rotation of a defect dipole in a mixed ionic compound is, therefore, influenced by the lattice constant modification (long-range effect). The rotation might also be affected by local short-range perturbation, caused by the spatial distribution of the substituting ions in the immediate neighborhood of the defect. The activation energy (which is identical to the migration enthalpy of the bound defect[2,3]) and the vibrating frequency of the moving entity, are functioned to the long-range phenomena, while, the short-range ones probably stimulate rotational modes involving new additional migration paths of the moving defect.

Recent work on the dielectric relaxation of mixed crystals is rather small in quantity and limited to simple crystal structure materials,[1,4–7] such as the alkali halides and alkaline-earth fluorides. Recently, we have focused on the ionic relaxation of the so-called calcite group crystals, consisting of calcite $CaCO_3$, magnesite $MgCO_3$, and dolomite $CaMg(CO_3)_2$, which all crystallize in the rhombohedral system.[8–10] The crystal structure of magnesite can be roughly approximated by that of NaCl, with Mg on the cation site and CO_3 on the anion site. Although the real unit cell is an acute rhombohedron, the vast majority of researchers prefer a hexagonal representation.[8] In both magnesite and calcite, the carbonate group consists of three oxygens located at the corners of an equilateral triangle and a carbon in the center. The bonding inside the carbonate group is covalent. The bonding between the magnesium cation and the carbonate unit is mainly ionic, although recent calculations showed a small but significant covalent contribution.[11] Apart from the aforementioned specific features of the rhombohedral structure, we also note that the mixed crystal of the calcite family (i.e., dolomite), consists of alternate calcium and magnesium layers and the carbon is shifted in relation to the three oxygens' plane. The combined variation of the length of the cation-oxygen bonds and the slight rotation of the carbonate unit in dolomite, results in small distortions of the cation-oxygen octahedra from the structure of pure magnesite and calcite.

The defect dipole relaxation in calcite and dolomite has been considered in our previously published work,[12–14] while the relaxation in magnesite is studied in the present work. We intend to relate the defect dipole relaxation to the specific type of Ca or Mg sublattice and to study the relaxation dynamics of each kind of relaxation mechanism. As an experimental tool, we employ the thermally stimulated depolarization current (TSDC) technique, which is a high-resolution dielectric relaxation spectroscopy method.[15] The relaxation mechanisms (dipole rotation, interfacial, and space-charge polarization) can, in principle, be recorded as distinct depolarization peaks in a TSDC spectra, even if the defect concentration is small. The origin of each mechanism can be identified by employing standard experimental TSDC schemes and the energy parameters can be evaluated accurately. Thus, the TSDC method can detect the defect structure indeed and probe any possible variation of the defect structure, which is related to any polarizable configuration, as a peak characterized by its location in the spectra, its

height and its energy parameters. It is the scope of the present paper to provide experimental TSDC results for magnesite ($MgCO_3$) and, by reviewing the results for calcite[13] ($CaCO_3$) and dolomite [$CaMg(CO_3)_2$],[12,14] to propose explanations for the relaxation observed in the calcite family. As will be discussed below, it seems that the models published up to date[1,4–6] do not fit the calcite family members.[8]

II. THEORY

The rotation of dipoles and the motion of free charge carriers under certain boundary conditions are responsible for the dielectric relaxation of an insulator.[15] The relaxation of dipoles in ionic materials involves the rotation of defect dipoles. On the other hand, the migration of free charges (under the action of an external electric field) can be impeded by obstacles existing in the bulk (i.e., dislocations or grain boundaries)[16] resulting in the interfacial polarization or by the non-Ohmic sample electrode interface leading to the space-charge formation. The temperature dependence of the relaxation time τ, which governs the relaxation process, is usually assumed to obey the exponential Arrhenius law:

$$\tau(T)=\tau_0\ \exp\left(\frac{E}{kT}\right), \tag{1}$$

where E denotes the activation energy, τ_0 is the preexponential factor and k is the Boltzmann's constant.

In the thermally stimulated depolarization current (TSDC) method the depolarization current emitted by a previously polarized dielectric, is recorded as a function of the increasing temperature of the sample.[17] The specimen is polarized at the temperature T_p for a time interval $t_p \gg \tau(T_p)$ and, subsequently, by keeping the external polarizing field on, we freeze to the liquid-nitrogen temperature (LNT), where the relaxation time is practically infinite. As a result, on removing the electric field, the dielectric remains polarized. The depolarization current is recorded via a sensitive electrometer, as the sample is heated at a constant heating rate b. At the temperature range where the thermal energy competes with the energy E needed for the reorientation of the polarized dipoles, we get a transient electric signal called the thermogram. Different types of dipoles, or the dispersion of the frozen space-charge polarization, stimulate additional peaks.

The depolarization current originating by the reorientation of noninteracting dipoles is

$$I(T)=\frac{S\Pi_0}{\tau_0}\exp\left[-\frac{E}{kT}-\frac{1}{b\tau_0}\int_{T_0}^{T}\exp\left(-\frac{E}{kT}\right)dT\right], \tag{2}$$

where Π_0 is the initial polarization of the dielectric, S is the sample's surface area which is in contact to the electrode and T_0 coincides with the LNT. The activation energy E is identical to the migration enthalpy h^m.[2,3]

The relaxation time τ is given by the following relation (area method):

$$\tau(T)=\frac{1}{bI(T)}\int_{T}^{T_f} I(T)dT, \tag{3}$$

where T_f is the final temperature of the peak where the current becomes null. For the initial part of the curve, Eq. (2) is approximated by

$$I(T)\cong\frac{S\Pi_0}{\tau_0}\exp\left(-\frac{E}{kT}\right). \tag{4}$$

For a linear heating rate b, the temperature $T_{\max}$ where the current has the maximum is given by the equation

$$\frac{T_{\max}}{\tau(T_{\max})}=\frac{Eb}{kT_{\max}}. \tag{5}$$

Equations (1) and (3) can lead to the evaluation of the activation energy E and the factor τ_0, through a $\ln\tau(1/T)$ plot. The initial rise data fitted to a $\ln I(1/T)$ straight line, also yields the evaluation of E, via Eq. (4).

If the activation energy is not single valued but has a Gaussian distribution around E_0, with distribution function[18,19]

$$f(E)=\frac{1}{\sqrt{2\pi}\sigma}\exp\left[-\frac{(E-E_0)^2}{2\sigma^2}\right], \tag{6}$$

where σ is the broadening parameter, the total depolarization current can be written

$$I(T)=\int_{-\infty}^{+\infty} f(E)I(T,E)dE, \tag{7}$$

where the term $I(T,E)$ is the monoenergetic TSDC equation [see Eq. (2)].

The integral of Eq. (2) can be approximated by the following analytical expression:

$$\int_{T_0}^{T}\exp\left(-\frac{E}{kT}\right)dT=\left.\frac{T\exp(-E/kT)(E/kT+3.0396)}{(E/kT)^2+5.0364(E/kT)+4.1916}\right|_{T_0}^{T}, \tag{8}$$

while the integration of Eq. (7) can be performed from 0 to $3E_0$.[18]

The distribution of the relaxation time may result from the distribution of the activation energy E, the preexponential factor τ_0, or both. The distribution can be prescribed and a modified TSDC equation can be constructed, in the way mentioned above, in order to analyze the data. The choice of the distribution function is rather arbitrary, so it is more advantageous to derive the distribution from the experimental data, if possible.[15] The initial rise edge of a distributed peak merely gives an estimate of the activation energy for the fast relaxation mechanisms. In order to evaluate the activation energy, except for the fast (low-temperature) mechanisms, but for the entire temperature region, we can carry out successive partial discharges of the mechanisms. Each initial

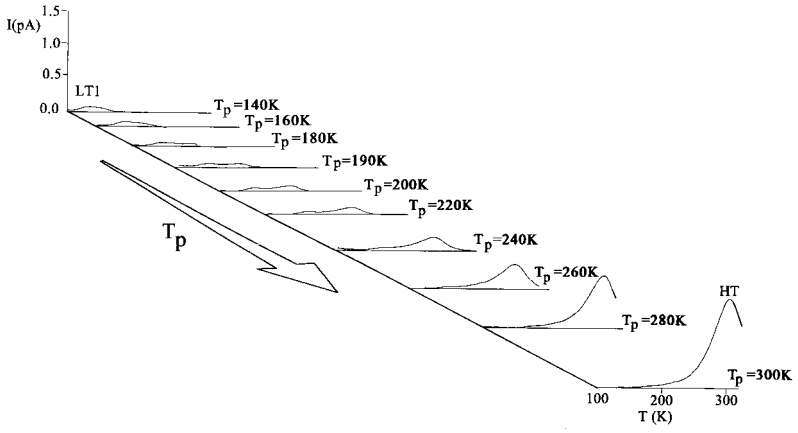

FIG. 1. Thermograms of polycrystalline magnesite obtained by varying the polarization temperature T_p. We used platinum electrodes. In all experiments the polarization conditions were: $E_p = 13.64$ kV/cm and $t_p = 2$ min. It is obvious that the polarization state of the HT mechanism strongly affects the LT1 mechanism.

rise can lead approximately to the evaluation of the activation energy for the mechanisms activating in the temperature region, where the current is recorded. The accuracy of this method is better for the temperature region close to the maximum of the initial peak.[15] The alternative experimental scheme is known as partial heating[20] and is presented in detail in Sec. IV.

III. EXPERIMENTAL DETAILS

The cryostat operates from the liquid-nitrogen temperature (LNT) up to 400 K. A vacuum better than 10^{-6} mbars, was created by an Alcatel molecular vacuum pump. The crystals were placed between platinum electrodes and were polarized by using a Keithley 246 dc power supply. The temperature was measured by means of a gold-chromel thermocouple connected to an Air-Products temperature controller. The temperature rise was monitored by the controller and the desired constant heating rate (around 3 K/min) was attained throughout each TSDC scan. The depolarization current was measured with a Cary 401 electrometer. The output signals from the controller and the electrometer were digitized via a Keithley DAS 8 PGA card installed into a computer. Afterwards the data were analyzed with the appropriate software we have developed.

Magnesite is the name of both single-crystal and polycrystalline $MgCO_3$ salts. The samples we studied come from the large deposits of compact polycrystalline magnesite located at the island of Euboea (Greece)[9] and their exhibiting feature is the white (snowlike) color. For this reason the common name of the material is leukolite. The analysis performed by the Institute of Geological and Mining Research (Greece) gave the following results: 47.90 wt % MgO, 2.80 wt % Si, 0.02 wt % Al, 0.13 wt % Fe, 0.41 wt % Ca, 0.02 wt % Mn, 0.02 wt % Sr, less than 0.01 wt % K, 0.04 wt % Na, and 0.31 wt % humidity.

IV. RESULTS AND DISCUSSION

Detection of the relaxation mechanisms activating at the low-temperature region

During a TSDC experiment, in general, the relaxation of dipoles can be affected strongly by the formation of space charge, provided that free charge carriers exist in the matrix. The space-charge polarization, which is formed during the polarization stage, results in an internal electric field, which opposes the external polarizing field. The total electric-field intensity can probably get a null value. Subsequently, the dipoles can either remain randomly oriented or the dipole polarization may be much weaker than that achieved in a sample which is free of space charges.[15,21] It is also probable that the dipole population undergoes a polarization process during the TSDC heating stage, because of the nonuniform spatial distribution of the space charge.[22] So, the TSDC thermogram might not be representative of the ionic relaxation occurring in the matrix; the location and the amplitude of the peaks would be, in principle, strongly changed or completely absent from the spectrum.

The vast majority of TSDC studies reported up to date employ the usual mode, which involves the polarization of the crystal at room temperature (RT). Recalling that the space charge mechanisms are activated at the RT region, it is wise to prohibit its formation by polarizing at temperatures T_p lower than RT, whereas the relaxation time $\tau(T_p)$ of the space-charge mechanism is significantly longer than the polarization time t_p. In this way, we may get a reliable picture of the low-temperature dipole relaxation.[14] In Fig. 1 we display a set of the thermograms obtained on a polycrystalline magnesite sample, which was polarized at various polarization temperatures T_p and keeping both the polarizing electric-field intensity E_p and the polarization time t_p constant. Starting from low-temperature polarization, we detect a unique low-temperature mechanism, labeled as LT1. As the polarization temperature augments, we record an additional intense peak labeled HT. The polarization of the HT mechanism leads obviously to the drastic alteration of the LT1 band. Detailed TSDC studies[23] proved that the HT band is related to the space-charge relaxation, so, the phenomenon is well interpreted by the aspects mentioned above. Hence, it is firmly established that the LT1 is actually the only relaxation mechanism appearing in the low-temperature spectrum. The proposal stemming from the latter results is that the appropriate selection of T_p is of great importance. In order to avoid frustrating conclusions, we have to select a low polarization temperature, instead of polarizing at RT.

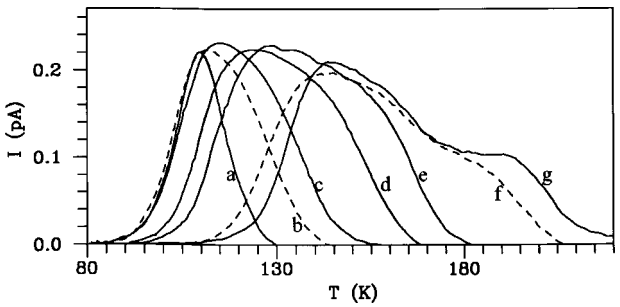

FIG. 2. Low-temperature spectra of polycrystalline magnesite obtained by changing the polarization temperature T_p. The polarization conditions were: $E_p = 62.50$ kV/cm and $t_p = 2$ min, while the electrode material was platinum. (a) $T_p = 100$ K, (b) $T_p = 115$ K, (c) $T_p = 125$ K, (d) $T_p = 135$ K, (e) $T_p = 150$ K, (f) $T_p = 170$ K, (g) $T_p = 180$ K.

Low-temperature dielectric characterization

We chose different polarization temperatures, in the temperature territory where the LT1 activates. We started from $T_p = 100$ K up to 180 K, by using platinum electrodes, while the other polarization parameters were kept constant ($E_p = 8.33$ kV/cm, $t_p = 2$ min) (Fig. 2). A plateaulike maximum of the thermocurrent, which is located around $T_{max} = 140$ K, is exhibited and does not shift, when T_p is higher than approximately 140 K. In the latter case, although there are apparent contributions of the HT mechanism to the end tail of LT1, the peak amplitude does not change. By polarizing at temperatures lower than 140 K, the maximum temperature is gradually lowered, with simultaneous gradual reduction of the total charge released. These results can be interpreted: (a) as the overlap of two or more distinct simple peaks, or, (b) as a unique relaxation mechanism characterized by distribution of the relaxation time values. Since the variation of the polarization conditions do not lead to distinct separate peak maxima, we would consider hypothesis (b) as the most probable to occur. This aspect will be justified later on by the results of the partial heating technique and the fitting analyses.

By polarizing at $T_p = 150$ K, we applied a field intensity of $E_p = 62.50$ kV/cm, for different polarization times $t_p = 2$, 4, and 8 min, by using platinum electrodes. The subsequent thermograms verified the polarization of the mechanism to saturation. This feature is typical of dipole relaxation mechanisms. In Fig. 3 we have plotted the peak amplitude I_{max} vs the polarizing field intensity E_p. The relation is linear and it seems that no saturation is achieved in the field range we used. Although dipole peaks provide linear $I_{max}(E_p)$ plots, the linearity does not imply the dipolar character of the mechanism.[16]

In our experiments, we employed platinum and bronze electrodes. For each kind of metal electrodes, we performed four successive scans, under exactly the same polarization conditions ($T_p = 150$ K, $E_p = 62.50$ kV/cm, and $t_p = 2$ min). The LT1 band was recorded adequately reproducible. The LT1 peak is not sensitive to the electrode material, implying the dipolar feature of the peak. We placed two thin teflon (insulating) foils between the sample surfaces and the electrodes, constructing the metal-insulator-sample-insulator-metal configuration.[15] The peak maximum was not influenced, supporting the aforementioned result that the LT1 band is a dipolar one. This conclusion was also supported when we varied the thickness of the specimen: Under the same polarization conditions ($T_p = 150$ K, $E_p = 26.31$ kV/cm, and $t_p = 2$ min) we performed experiments for two different sample thicknesses: 1.14 and 0.65 mm. The invariance of the LT1 signal indicates that the polarization of the LT1 is homogeneous and typical of dipole polarization.

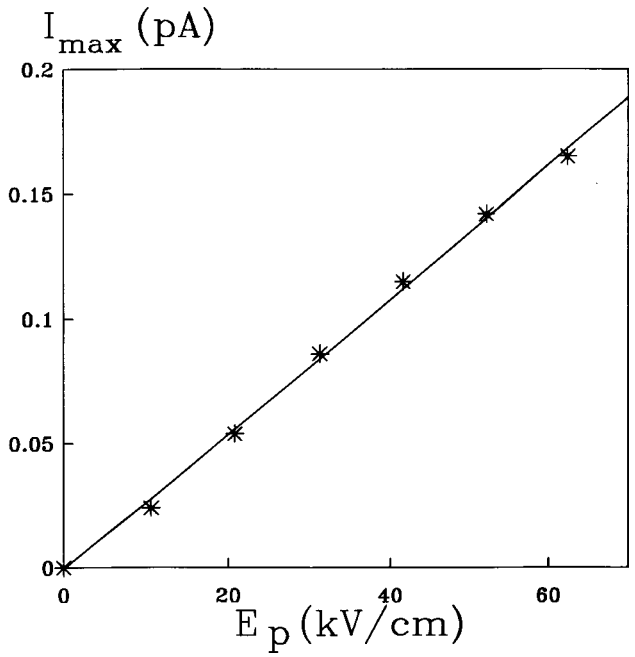

FIG. 3. Dependence of the LT1 signal amplitude upon the polarization field intensity E_p by using platinum electrodes. The polarization conditions were: $T_p = 150$ K and $t_p = 2$ min.

In order to have more information about the nature of the dipoles which stimulate the LT1 band, we have thermally treated a sample. In Fig. 4 we present the thermogram recorded in an as-received specimen, together with the spectrum recorded after the annealing at 400 °C for the time interval of 30 min and subsequent quench to RT. In both

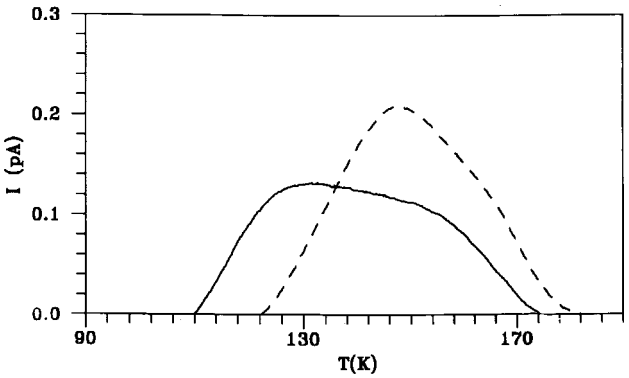

FIG. 4. The effect of the thermal treatment on the LT1 band of the polycrystalline magnesite. The solid line comes from a received (virgin) sample, while the dashed line was recorded after annealing at 400 °C for 30 min and subsequent quench to RT. In both cases the polarization conditions were $T_p = 150$ K, $E_p = 46.15$ kV/cm and $t_p = 2$ min.

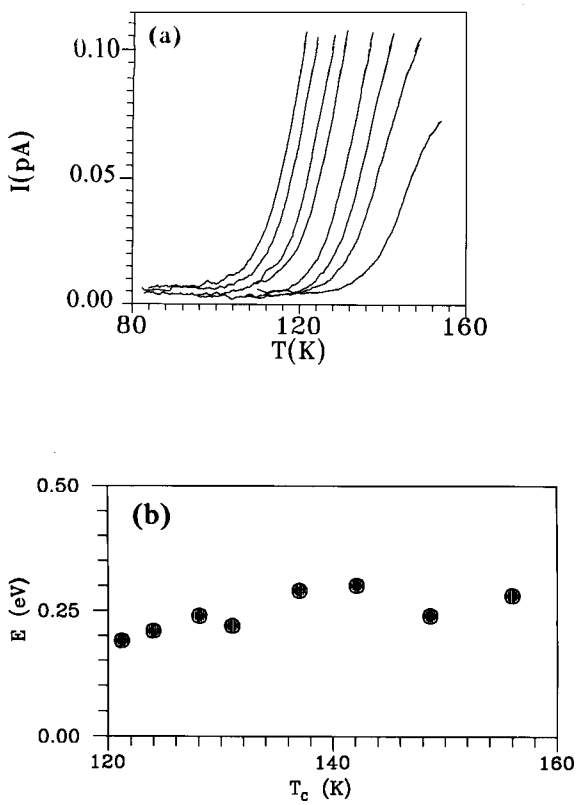

FIG. 5. (a) Initial rise thermocurrent curves recorded in polycrystalline magnesite by employing the partial heating scheme. (b) Temperature distribution of the activation energy E of the LT1 band appearing in the magnesite's spectra obtained by the partial heating scheme.

experiments, the polarization conditions were $T_p = 150$ K, $E_p = 46.15$ kV/cm, and $t_p = 2$ min. The band is shifted about 8 K towards higher temperature and the signal amplitude is augmented. The area under the current curve, which is proportional to the total number of dipoles, increases to approximately 16%. The sensitivity to the thermal perturbation indicates that the band is related to defect dipoles. The augmentation of the band area indicates that (i) the equilibrium state (virgin state) of the defect structure is related to large agglomerate configurations, which decompose to smaller units, or, (ii) the thermal modification of the virgin dipole structure involves slight changes of their configuration. If speculation (i) was true, we should detect the reduction of LT1 and the simultaneous appearance of a new mechanism, which corresponds to the liberated dipole population; the new dispersion should activate far from the temperature region where the virgin spectrum is recorded because the new dipole configuration would be radically different. The observation that the LT1 band is itself changed, is rather interpreted via assumption (ii).

Evaluation of the energy parameters of the LT1 band

The shape of the LT1 band deviates from the shape of an asymmetric signal, which a population of noninteracting dipoles stimulates. The deviation is somehow expected from the experimental result mentioned in the preceding subsection: the band shifts to lower temperatures on reducing the

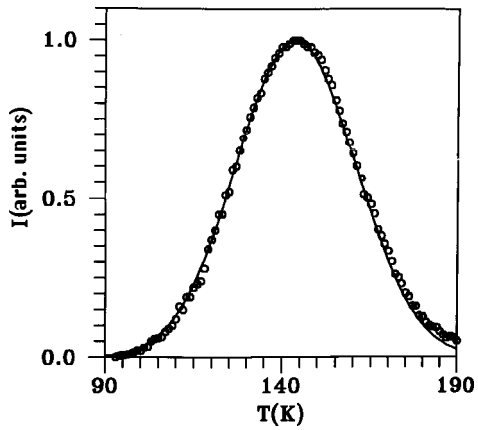

FIG. 6. Theoretical curve with Gaussian distribution in the activation energy (solid line) fitted to the experimental points (circles). The dispersion was fully polarized by polarizing at the maximum ($T_p = 140$ K) for a short time interval ($t_p \approx 2-3$ s) in order to minimize the space-charge contribution. The energy parameters of the theoretical curve are: $E_0 = 0.220$ eV, $\sigma = 0.023$ eV, and $\tau_0 = 4.787 \times 10^{-6}$ s.

polarization temperature T_p, for $T_p < 140$ K. This implies that the mechanism is characterized by the distribution in the relaxation time. However, it is not possible to state if the distribution in the relaxation time arises from the distribution in the activation energy E, in the pre-exponential factor τ_0, or both. We estimated the activation energy values by the direct experimental technique of the partial heating.[20] This alternative experimental scheme consists of polarizing the relaxation mechanism to saturation and cooling down to the LNT. In the heating depolarization procedure, as soon as we record the initial part of the depolarization current, we stop the heating at a temperature T_c and cool down to the LNT immediately afterwards. A second successive heating to a temperature T_c, higher than the previous one, will give another initial depolarization curve. The procedure is repeated until the LT1 band is completely discharged, providing a set of initial rise curves [Fig. 5(a)]. Equation (4) can be fitted to the initial rise data and provide an approximate value of E. The resolution and the accuracy of the method have been discussed in Sec. II. In an E vs T_c diagram [Fig. 5(b)] we see that the values range from 0.19 to 0.30 eV. The distribution is rather narrow. We can hardly say that the activation energy values accumulate around two distinct values. In combination with the fact that two different maxima were not obtained when we varied the polarization conditions, we can probably exclude the possibility of two overlapping peaks.

In addition to the partial heating, we performed a fitting procedure on the thermograms obtained in the usual manner. In order to obtain the complete energy spectrum of the mechanism, the relaxation mechanism has to be fully polarized. The complete polarization is achieved by polarizing at the temperature T_p higher or equal to the maximum of the peak. As can be seen in Fig. 2, by selecting such a polarization temperature the end tail of the LT1 band suffers from space-charge contributions. The peak depicted in Fig. 6 was obtained by polarizing at the maximum of the peak ($T_p = 140$ K) for a short time interval ($t_p \approx 2-3$ s). Although the true polarization time is not actually controlled (the time

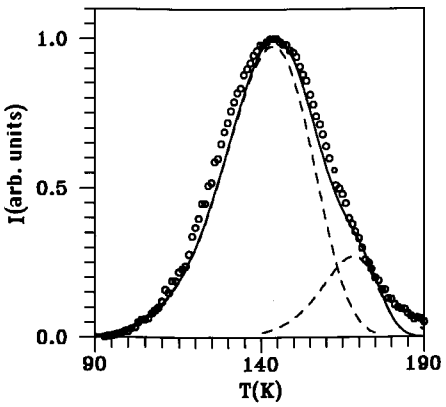

FIG. 7. Theoretical curve (solid line) which best matches the experimental data (circles) assuming that the LT1 band is composed by two single overlapping peaks. The two components are also depicted (dashed line). The energy parameters, for the low-temperature component, are $E=0.121$ eV, $\tau_0=1.719\times10^{-2}$ s, and $E=0.269$ eV, $\tau_0=1.540\times10^{-6}$ s, for the high-temperature one.

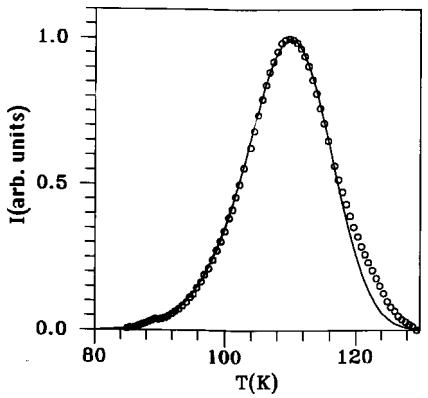

FIG. 8. Theoretical curve with Gaussian distribution in the activation energy (solid line) fitted to the experimental points (circles). The band was recorded by polarizing at $T_p=100$ K. The parameters of the theoretical curve are $E_0=0.200$ eV, $\sigma=0.007$ eV, and $\tau_0=8.960\times10^{-6}$ s.

needed to cool the sample with the electric field on, is comparable to the time interval t_p), the result is a cleaned peak, with well-defined maximum and smother than the dispersions presented in Fig. 2. We adopted the most usual assumption that the activation energy values obey a Gaussian distribution around a mean value E_0, while τ_0 remains constant. The experimental curves were fitted to Eq. (7) and a set of E_0, σ, and τ_0 was obtained through a nonlinear least-squares procedure. The results of the computational process were visually examined so as to check if there exists a good match in the low-temperature part of the curve. In Fig. 6 we present the experimental data of the LT1 peak together with a theoretical curve with relaxation parameters $E_0=0.220$ eV, $\sigma=0.023$ eV, and $\tau_0=4.787\times10^{-6}$ s.

It is now worth comparing the Gaussian fit results to the partial heating ones. The low intensity of the depolarization current urged us to record only eight partial heating discharges and sample a few energy values. Thus, it is difficult to determine whether the partial heating energy span is centered around a mean value. We also note that the width of the energy distribution obtained from the partial heating is about five σ. The gap between 0.19 eV and E_0 is about 1.5 σ, while the difference between the 0.30 eV and E_0 is about 3.5 σ. The question that arises is whether there is a discrepancy between the results of the partial heating and those of the Gaussian fit. First, the 0.19 eV value is well sited within the energy band determined by the Gaussian fit. The mechanism related to the 0.19 eV value is not as strong as that corresponding to E_0. Subsequently, the 0.19 eV signal should be weaker than those from the intermediate region. In fact, the 0.19 eV depolarization curve does not correspond to a unique mechanism. The signal is strongly assisted by the neighboring high-temperature mechanisms. As stated in Sec. II, this is exactly a reason why the partial heating directs to approximate energy values. Consequently, the 0.19 eV signal should be relatively strong, in agreement with the situation presented by Fig. 5(a). The end signal of the partial heating corresponding to the high-temperature mechanisms is weaker than the signals from the intermediate region [see Fig. 5(a)]. The high-temperature region suffers from the space-charge contribution (HT peak), so, the 0.30 eV signal includes a spurious current contribution. For this reason the signal is not dramatically weak and the energy value obtained should be higher than the real value for the slow dipole components. We assert that the partial heating and the Gaussian fit provide comparable energy spectra.

Alternatively, the broad LT1 relaxation can be considered as being the overlap of two single relaxations. The experimental evidence opposes this aspect; the variation of the polarization conditions did not reveal two distinct maxima and the partial heating energies did not indicate the existence of two single peaks. However, we also tried a least-squares fit with the model of two overlapping single mechanisms. The result was a set of different peaks, which could hardly account for the broad experimental dispersion. A visual inspection showed that the theoretical curves could not match the data points well. In Fig. 7 we show one of the best theoretical curves. The two overlapping single peaks are also depicted. We see that the rising part of the two-peak theoretical curve does not match the data points. There is also deviation at the high-temperature region. The parameters for the first peak, which reaches a maximum at 144 K, are $E=0.121$ eV, $\tau_0=1.719\times10^{-2}$ s, and $E=0.269$ eV, $\tau_0=1.540\times10^{-6}$ s, for the second one, which reaches a maximum at 168 K. The relative intensities (in comparison to the amplitude of the LT1 band) are 0.96 and 0.27, respectively. The energy for the first mechanism is low and the preexponential factor is so unreasonably large that it is rather physically unacceptable. By comparing Fig. 6 to Fig. 7, we conclude that the LT1 band is best described by the unique relaxation with distribution in the activation energy. We note that a series of additional iterations, by employing the two-peak model, did not reduce the discrepancy between the theoretical and experimental curves.

In Fig. 8, a curve obtained by polarizing at $T_p=100$ K is depicted, together with the theoretical curve that best matches the experimental data. The energy parameters of the theoretical curve are $E_0=0.200$ eV, $\sigma=0.007$ eV, and $\tau_0=8.960\times10^{-8}$ s. The energy spectrum is a low energies' subset of the energy spectrum that we got from the analysis

of the fully polarized peak (Fig. 6). This result was expected, since the selection of the polarization temperature prohibited the polarization of the high-energy mechanisms. For the same reason, the broadening parameter σ is suppressed. It is worth examining the validity of the Gaussian fitting by pointing out the following: (i) Even though the polarization temperature $T_p = 100$ K is low enough to warrant an efficient peak cleaning, the end tail of the theoretical curve can hardly match the experimental curve, and (ii) The pre-exponential factor τ_0 is about two orders of magnitude smaller than the value obtained from the analysis of the fully polarized peak. It is probable that the pre-exponential factor τ_0 is not single valued but it is distributed. This aspect may explain the broadening of the bands, which are depicted in Fig. 2. On the other hand, let us suppose that the broadening of the TSDC curves and the difficulty in achieving an adequate match of the theoretical curve to the end tail data, is caused by the overlap of two different peaks. Then, the selection of the extreme polarization temperature $T_p = 100$ K should lead to the isolation (cleaning) of the first component mechanism and, subsequently, the end tail data of the peak depicted in Fig. 8, should match well to the theoretical curve. This does not occur and the aspect that the τ_0 values are also distributed, seems quite probable.

V. COMPARATIVE STUDIES OF THE DEFECT DIPOLES IN THE CALCITE FAMILY SALTS

The LT1 and LT2 dispersions in the calcite-type crystals

The results for polycrystalline magnesite, which are presented in this paper, can critically be discussed by reviewing the recent results of calcite[13] ($CaCO_3$) and dolomite [$(CaMg(CO_3)_2$] (both single crystal and polycrystalline).[12,14] In this way, we may obtain an overall view of the defect dipole formation and the dipole dynamics in the rhombohedral crystal structures. The temperature T_{max} where a peak reaches a maximum, the values of the energy parameters (E and τ_0) and the relaxation features (i.e., the dependence upon the sample thickness) are specific exhibiting characteristics of a relaxation mechanism. In this sense, the relaxation spectra for a family of materials can be attributed to their specific structural features. Additionally, the thermograms can monitor the changes in the defect structure induced by some kind of perturbation (thermal anneal, irradiation, or mechanical treatment).

Following the above-mentioned criteria for identifying and relating the relaxation mechanisms in a certain set of materials, we can point out that the LT1 band has also been detected in dolomite,[12,14] while it is absent in the spectra of single-crystal calcite.[13] Especially, by comparing the results for dolomite to those reported in this paper, we note the following for the LT1 band:

(a) The temperature where the current has a maximum is practically the same, although the maximum is plateaulike in magnesite.

(b) The relaxation energy values, which were obtained by the partial heating, are distributed from 0.24 to 0.40 eV for dolomite[14] and 0.19 to 0.30 eV for magnesite. The difference in the activation energy values is attributed to the fact that the environment around the LT1 entities, is modified by the presence of the additional Ca ions in dolomite.

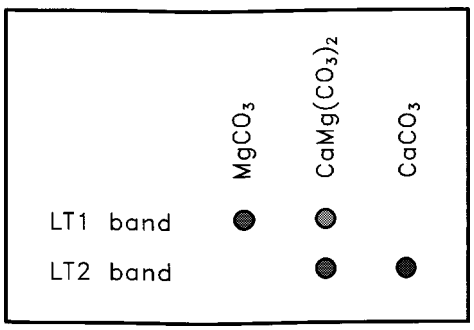

FIG. 9. Schematic representation which depicts the presence of the LT1 and LT2 bands in the TSDC spectra of the calcite group members.

(c) The thermal treatment exerted on dolomite was the same as that mentioned above, but the result was a shift to lower temperatures.[14] The discrepancy with the situation observed in magnesite shows that the LT1 population drives the system to two different perturbed states, each one influenced by the specific lattice type.

Another intense peak (labeled LT2), which reaches a maximum at about 188 K has been found in the thermograms of dolomite and calcite. In the present work, we tried many different polarization temperatures, so as to ensure that no other peak (apart from LT1) is activated in the vicinity of 188 K. According to the experimental results, the LT2 band is definitely absolutely absent in the magnesite's spectra. Figure 9 denotes the LT1 and LT2 mechanisms appearing in the relaxation spectra of the calcite group members. We point out that the LT1 mechanism is related to the $MgCO_3$ lattice and the LT2 to the $CaCO_3$ lattice. In dolomite, where the $CaCO_3$ and $MgCO_3$ sublattices constitute the matrix material, both LT1 and LT2 appear in the relaxation spectra.

It is now important to examine two hypotheses: (a) LT1 and LT2 are the result of two different modes of relaxation of the same defect dipole configuration,[1] (b) LT1 and LT2 correspond to the relaxation of two different types of dipoles. Speculation (a) assumes that the lattice variation (the lattice constant change and the local effect produced by the mixing of Mg and Ca cations) assists the dipole rotation via different migration paths, with different energy parameters (E and τ_0). As a result, a different peak maximum should appear, in accordance with Eq. (5). However, the exhibiting difference between the two mechanisms (apart from the large difference in the activation energy values) is that the LT1 mechanism is determined by the distribution in the relaxation time. This indicates that the nature of the relaxation procedure drastically diverges from the simple relaxation of noninteracting dipoles (unique relaxation time mechanism), which characterizes LT2, as reported in Ref. 14. We can therefore direct to hypothesis (b); i.e., that the LT1 and LT2 peaks stimulate from the reorientation of two distinct types of dipoles.

Our proposal is different from the usual interpretation that the lattice variation perturbs the rotational dynamics of the defect dipole;[1] we speculate that the $CaCO_3$ sublattice favors the formation of LT2 dipoles and the $MgCO_3$ sublattice, the LT1 ones. The formation of the specific type of defect structure is determined by the necessity for minimization of the Gibbs free energy of the crystal (equilibrium state). This aspect is justified by the thermal perturbation results: The vir-

gin state is an equilibrium one, characterized by its high stability. So, it is very difficult to drive the system to a metastable position, since both LT1 and LT2 (see Refs. 12–14) survive the thermal anneal, although they are modified in the shape, while, no other additional aggregate is recorded in the TSDC spectra of the annealed samples. If the equilibrium was a near one, then the thermal treatment would decompose the LT1 dipoles, and, subsequently, new peaks would appear in the spectrum.

Attribution of the relaxation mechanisms

In the present paragraph we shall try to trace the identity of the defects participating in the dipoles, by taking into account the impurity content of the materials, starting from the LT1 band. It is well known that Mn^{2+} is a widespread impurity in the carbonate salts[24,25] and is incorporated by preferential substitution of the Mg^{2+} ions, rather than the Ca^{2+} ones.[26] Thus, the LT1 band might be related to the appearance of Mn^{2+} in the $MgCO_3$ lattice. It is difficult to speculate about the dipole configuration, in the frame of local charge compensation; by accepting that the Mn^{2+} is incorporated into the matrix substitutionally, no electrical charge compensation is needed. Consequently, the Mn^{2+} impurity does not act as a center for impurity-vacancy dipole formation. Furthermore, we may assume that the Mn^{2+} ion serves as the linking defect between the dipole agglomerates and the Mg sublattice. It is also probable that charge compensation occurs by nonlocal charge compensation of statistical nature.[26]

A more sophisticated explanation can be proposed, recalling that the temperature region where LT1 activates (around 140 K) is characteristic for materials containing water in their structure.[27] Recent infrared experiments performed on magnesium carbonate compounds, indicated the presence of OH bonds, either from hydroxyl ions or water molecules and proved that the magnesium sublattice can host hydroxyl.[28] So, it is probable that the LT1 is related to the rotation of defect dipoles, with hydroxyl or water molecules as the major participant. The situation that the relaxation is caused by the rotation of water molecules, probably located at the interfaces of the crystallites or grains, seems rather weak. In this case, the LT1 band would also appear in (polycrystalline) calcite, but this does not occur.[13] The defect dipoles of this type must actually be bulk ones and are strongly bound to the lattice, because the total number (expressed by the charge released during the depolarization stage) is not reduced after the thermal anneal. The latter situation (the stability of the total amount of dipole population) was also observed in dolomite,[14] indicating that the hydroxyl complexes settle into the $MgCO_3$ lattice firmly. The changes of the band's shape and position, which accompany the thermal anneal, can be explained by the structural configuration changes induced by the thermal perturbation. It is worth noticing that the observation of the LT1 band, both in magnesite and dolomite (which are materials coming from different localities and developed under different forming conditions), denotes that the virgin defect structure is a stable equilibrium one, while the states achieved after the perturbation, are rather metastable, an aspect especially exhibited in dolomite (See Ref. 14).

We now proceed with the understanding of the item that the LT2 band is absent from the magnesite spectrum, while it appears in the spectra of the materials where the Ca sublattice exists. Strontium (Sr^{2+}) is a widespread impurity found in the alkaline-earth carbonate salts.[29] It is reasonable to assume that strontium is hosted up interstitially by the calcite and dolomite matrices. For each impurity cation, the total excess charge is $+2|e|$, where e denotes the electron's charge, which is compensated by the creation of one cation vacancy (either calcium or magnesium vacancy), for reasons of total charge neutrality of the crystal, with $-2|e|$ effective electric charge. The electrostatic attraction between Sr^{2+} and the cation vacancy can lead to the formation of a defect dipole, with length equal to one interatomic spacing. These impurity-vacancy dipoles, or, some larger clusters may be responsible for the stimulus of the LT2 band, in the calcite and the dolomite spectra. The hexagonal unit-cell volume of magnesite is the smallest one (279.05 $Å^3$) in comparison to dolomite (321.60 $Å^3$) and calcite (367.85 $Å^3$),[30] indicating that the available ''interstitial volume'' in magnesite is relatively the smaller one. Nevertheless, it would be energetically favorable for the magnesite matrix, to host up the Sr^{2+} impurity into a cation lattice site, because this defect location would probably minimize the lattice distortion caused by the doping. Since strontium and magnesium cations are of the same valence, there is no necessity for charge compensation by cation vacancy creation and, subsequently, the LT2 centers would not exist.

VI. CONCLUSION

A unique low-temperature relaxation mechanism (labeled LT1) of polycrystalline magnesite has its maximum around 140 K in the thermal depolarization spectrum. Extensive experimental schemes indicated that the mechanism is related to a defect dipole population, with distribution in the relaxation time, while no other dipolar mechanism operates. Especially, a band (labeled LT2), which was recorded in the thermograms of both calcite and dolomite, is definitely absent in the spectrum of magnesite. By reviewing our previous results for calcite and dolomite, we stated that the LT1 mechanism corresponds to the specific defect structure favored by the Mg sublattice and the LT2 one, to the Ca sublattice. The common interpretation that the same dipole relaxes through different modes, which are induced by the mixed crystal-lattice changes, does not apply to the calcite group salts. The defect dipoles which stimulate the LT1 mechanism, might be composed of Mn ions or, most probably, by water molecules or hydroxyl ions. The LT2 band, which is absent in magnesite even though it is detected in calcite and dolomite, might be related to two different ways of divalent Sr incorporation, depending on the host environment; the substitution of a host cation needs no charge compensation and, therefore, no defect dipole should be formed. On the contrary, the interstitial one demands the creation of a cation vacancy.

[1] R. Robert, R. Barboza, G. F. L. Ferreira, and M. Ferreira de Souza, Phys. Status Solidi B **59**, 335 (1973).
[2] P. Varotsos and K. Alexopoulos, J. Phys. Chem. Solids **41**, 443 (1980).
[3] P. A. Varotsos and K. D. Alexopoulos, in *Thermodynamics of Point Defects and Their Relation with Bulk Properties*, edited by S. Amelinckx, R. Gevers, and J. Nihoul (North-Holland, Amsterdam, 1985).
[4] S. C. Zílio and M. de Souza, Phys. Status Solidi B **80**, 597 (1977).
[5] T. Ohgaku and N. Takeuchi, Phys. Status Solidi A **42**, K83 (1977).
[6] A. Clark, R. Perez, R. Aceves, A. Hernádez, and O. J. Rubio, Cryst. Lattice Defects Amorphous Mater. **14**, 91 (1987).
[7] M. V. S. Sarma and S. V. Suryanarayana, J. Mater. Sci. **1**, 182 (1990).
[8] R. J. Reeder, in *Crystal Chemistry of Rhombohedral Carbonates*, Reviews in Mineralogy, Vol. 11, Carbonates: Mineralogy and Chemistry, edited by R. J. Reeder (Mineralogical Society of America, Washington, DC, 1983), p. 1.
[9] M. H. Battey, *Mineralogy for Students* (Longman, London, 1981).
[10] W. A. Deer, R. A. Howie, and J. Zussman, *An Introduction to the Rock Forming Minerals* (Longman, Essex, 1966).
[11] M. Catti, A. Pavese, R. Dovesi, and V. R. Saunders, Phys. Rev. B **47**, 9189 (1993).
[12] A. N. Papathanassiou, J. Grammatikakis, V. Katsika, and A. B. Vassilikou-Dova, Radiat. Eff. Defects Solids **134**, 247 (1995).
[13] N. G. Bogris, J. Grammatikakis, and A. N. Papathanassiou, in *Proceedings of the XII International Conference on Defects in Insulating Materials ICDIM92* (Germany, 1992), edited by O. Kanert and J.-M. Spaeth (World Scientific, Singapore, 1993), p. 804.
[14] A. N. Papathanassiou and J. Grammatikakis, Phys. Rev. B **53**, 16 252 (1996).
[15] J. Vanderschueren and J. Gasiot, in *Thermally Stimulated Relaxation in Solids*, edited by P. Braunlich (Springer-Verlag, Berlin, 1979).
[16] A. N. Papathanassiou, J. Grammatikakis, and N. Bogris, Phys. Rev. B **48**, 17 715 (1993).
[17] C. Bucci and R. Fieschi, Phys. Rev. Lett. **12**, 16 (1964).
[18] J. P. Calame, J. J. Fontanella, M. C. Wintersgill, and C. Andeen, J. Appl. Phys. **58**, 2811 (1985).
[19] E. Laredo, M. Puma, N. Suarez, and D. R. Figueroa, Phys. Rev. B **23**, 3009 (1981).
[20] R. Creswell and M. Perlman, J. Appl. Phys. **41**, 2365 (1970).
[21] Wang Da Yu and A. S. Nowick, Phys. Status Solidi A **73**, 165 (1982).
[22] N. Suarez, M. Puma, E. Laredo, and D. Figueroa, Cryst. Lattice Defects Amorphous Mater. **15**, 283 (1987).
[23] A. N. Papathanassiou, Ph.D. thesis, University of Athens, 1995.
[24] G. Calas, *Electron Paramagnetic Resonance*, Reviews in Mineralogy Vol. 18, Spectroscopic methods in Mineralogy and Geology, edited by F. C. Hawthorne (Mineralogical Society of America, Washington, 1988).
[25] A. B. Vassilikou-Dova and G. Lehmann, Fortschr. Mineral. **65**, 173 (1987).
[26] F. Prissok and G. Lehmann, Phys. Chem. Miner. **13**, 331 (1986).
[27] P. Pissis, D. Anagnostopoulou-Consta, L. Apekis, D. Daoukaki-Diamanti, and C. Christodoulides, J. Non-Cryst. Solids **1174–1181**, 131 (1991).
[28] F. T. Mackenzie, W. D. Bischoff, F. C. Bishop, M. Loijens, J. Schoonmaker, and R. Wollast, in *Magnesian Calcites: Low Temperature Occurrence, Solubility and Solid-Solution Behaviour*, Reviews in Mineralogy, Vol. 11, Carbonates: Mineralogy and Chemistry (Ref. 8), p. 97.
[29] J. Veizer, in *Trace elements and isotopes in sedimentary carbonates*, Reviews in Mineralogy, Vol. 11, Carbonates: Mineralogy and Chemistry (Ref. 8), p. 265.
[30] H. Effenberger, K. Mereiter, and J. Zemann, Z. Kristallogr. **156**, 233 (1981).